

# GLOBAL HEALTH

## Characterization of Polymorph Transformations That Decrease the Stability of Tablets Containing the WHO Essential Drug Mebendazole

MARIUS BRITS,<sup>1</sup> WILNA LIEBENBERG,<sup>2</sup> MELGARDT M. DE VILLIERS<sup>3</sup>

<sup>1</sup>Research Institute for Industrial Pharmacy and CENQAM, North-West University, Potchefstroom 2520, South Africa

<sup>2</sup>Unit for Drug Research and Development, Faculty of Health Sciences, North-West University, Potchefstroom 2520, South Africa

<sup>3</sup>School of Pharmacy, University of Wisconsin, 777 Highland Avenue, Madison, Wisconsin 53705

Received 2 June 2009; revised 7 July 2009; accepted 13 July 2009

Published online 18 August 2009 in Wiley InterScience (www.interscience.wiley.com). DOI 10.1002/jps.21899

**ABSTRACT:** This study investigated the influence of moisture and heat on the stability of mebendazole polymorph C in tablets. The polymorphic forms of mebendazole display significant differences in solubility and therapeutic efficacy and form C is preferred clinically due to its optimal bioavailability and reduced toxicity. An accelerated stability study of the polymorphs revealed that the Johnson–Mehl–Avrami–Erofev–Kolmogorov (JMAEK) model best described the kinetics of the solid-state transformation of form C to A. Rate constants obtained using this model was used to calculate half-lives and shelf lives of products stored under ICH conditions of 30°C + 65% RH and 40°C + 75% RH. Results showed that form C was converted to the thermodynamic stable, least soluble form A with increased temperatures and moisture, and at constant temperature and relative humidity this transformation was significantly increased when trace amounts of form A was present in the tablets. Four out of the seven products tested contained trace amounts of form A. In some tablets, the transformation to form A was so quick that it reduced the shelf life to less than 1 month. The tablet dissolution of these products was reduced to such an extent that it did not comply with USP and FDA specifications. © 2009 Wiley-Liss, Inc. and the American Pharmacists Association *J Pharm Sci* 99:1138–1151, 2010

**Keywords:** mebendazole; polymorph; stability; tablets; dissolution; kinetics; transformation

### INTRODUCTION

It is estimated that more than 3 billion people are infected by worms in the world today.<sup>1,2</sup>

Especially, the infections caused by nematodes are among the most prevalent communicable diseases, affecting more than 1 billion individuals. Children are particularly susceptible and in developing countries, parasitic nematodes are one of the major causes of childhood malnutrition, physical growth retardation, and deficits in cognitive and intellectual development. For example, a recent analysis of the association between hookworm and anemia in school-age children

Correspondence to: Melgardt M. de Villiers (Telephone: 608-890-0732; Fax: 608-262-5345; E-mail: mmdevilliers@pharmacy.wisc.edu)

*Journal of Pharmaceutical Sciences*, Vol. 99, 1138–1151 (2010)  
© 2009 Wiley-Liss, Inc. and the American Pharmacists Association

in Zanzibar suggested that 25% of all anemia cases, 35% of iron-deficiency anemia cases, and 73% of severe anemia cases could be attributed to hookworm infection.<sup>3</sup> Iron-deficiency anemia can affect the mental and motor development of children.<sup>4</sup>

For these reasons the WHO recommends the mass treatment of all children with anthelmintic drugs when the prevalence of infection with intestinal worms is greater than 50%.<sup>5</sup> The four anthelmintic drugs recommended for treatment of intestinal worms are albendazole, mebendazole, levamisole, and pyrantel.<sup>6</sup> Among these the benzimidazole, mebendazole, is especially useful because several studies that examined its use in children aged from 6 to 59 months reported no incidence of serious adverse experiences, and side effects were negligible.<sup>7,8</sup>

Mebendazole can exist as polymorphs and solvates in the solid state.<sup>9–11</sup> Of particular importance is the differences in the physicochemical properties of the three known polymorphs A, B, and C.<sup>10,12,13</sup> For example, the difference in solubilities of these polymorphs in physiologically relevant media is  $B > C > A$ . However, due to the increased toxicity of the highly soluble form B, form C is clinically preferred because its solubility is sufficient to ensure optimal bioavailability.<sup>14–17</sup> This is important because polymorph A has no anthelmintic activity alone or when present above 30% in polymorphic mixtures.<sup>15,17</sup>

Evans et al.<sup>18</sup> in a letter published in the *South African Medical Journal* asked that regulating authorities require testing to ensure that all batches of mebendazole raw material and tablets contain crystal polymorph C. However, such a test is still not required in any of the world's major pharmacopeia. In fact, the toxic form B and ineffective form A are still found in raw materials

and products.<sup>19–20</sup> If one assumes that manufacturers of mebendazole raw materials and products always use the active crystal form then one reason for the occurrence of the unwanted forms could be crystal transformations that occur postmanufacturing. To test this hypothesis this study looked at the stability of mebendazole polymorphs both as powders and in commercially available tablets.

## EXPERIMENTAL PROCEDURES

### Materials

Mebendazole polymorph C (batch number: F10958, Rolab, Pretoria, South Africa) and polymorph B (batch number: MWB/M-007/2006, Exim-Pharm International, Mumbai, India) were identified among raw material batches obtained from various manufacturers.<sup>19</sup> Polymorphs A, B, and C were also prepared as described earlier.<sup>11,13,21,22</sup> Physicochemical and spectral properties of the three mebendazole polymorphs are listed in Table 1. Commercially available mebendazole tablets were obtained from seven manufacturers in South Africa and randomly numbered, products 1–7, to conceal product identity. Table 2 provides a summary of the properties of the products.

The total moisture content of the various products was below 5% as determined by Karl Fisher titration. The total % water-soluble excipients (WSEs; %, w/w) in each product were determined. The initial mass of a tablet was determined ( $m_0$ ). The tablet was then transferred into a glass beaker containing 100 mL of distilled water and sonicated for 10 min to allow the WSEs to dissolve in the water. The solution was filtered and the dried mass of the water-insoluble matter

**Table 1.** Physicochemical and Spectral Properties of the Three Mebendazole Polymorphs

Form	IR (cm <sup>-1</sup> )		XRPD (°2θ)		Solubility at 30°C (mg/mL)		DSC	
	-NH	>C=O	Unique	100% <i>I</i> / <i>I</i> <sub>0</sub>	0.1 M HCl	0.1 M HCl + 1% SLS	<i>T</i> <sub>m</sub> (°C)	Δ <i>H</i> (kJ/mol)
A	3370	1730	7.67	7.67	0.02 ± 0.005	0.11 ± 0.006	244	232
B	3340	1700	5.84	19.07	0.07 ± 0.004	0.14 ± 0.007	223	181
							235	87
C	3410	1720	4.93	19.80	0.04 ± 0.003	0.12 ± 0.008	212	58
							240	172

For IR identification the stretching frequencies of the carbonyl (carbamate) and amine N–H stretch are listed. Solubility was measured in 0.1 M HCl and the USP dissolution medium for mebendazole tablets that contains sodium lauryl sulfate (SLS).

**Table 2.** The Properties of the 100 mg Mebendazole Tablets, Including the Percentage of Water-Soluble Excipient (WSE) and Water-Insoluble Excipient (WISE)

Product	Mebendazole Content (mg/tab)	Polymorph	Moisture Content (% w/w)	Average Tablet Weight (mg)	Filler	WSE (% w/w)	WISE (% w/w)
1	105.5	C (traces A)	4.37	288.7	Microcrystalline cellulose	3.62	59.85
2	103.5	C	3.89	298.0	Microcrystalline cellulose	1.34	63.93
3	99.9	C (traces A)	2.50	302.3	$\alpha$ -Lactose monohydrate	12.15	54.79
4	101.5	C	4.19	317.0	$\alpha$ -Lactose monohydrate	12.02	55.95
5	100.4	C (traces A)	1.82	301.7	Unknown	13.29	53.41
6	101.0	C (traces A)	2.66	313.4	Microcrystalline cellulose	0.52	67.27
7	101.9	C	3.93	350.6	$\alpha$ -Lactose monohydrate	16.01	54.92

Based on tablet weight and content analysis, the mebendazole occupied about 30–37% of the tablet weight.

( $m_i$ ) was determined. The total % WSE in each product was calculated using the following equation:

$$\%WSE = \frac{m_0 - m_i}{m_0} \times 100 \quad (1)$$

The mebendazole content, %WSE, and % water-insoluble excipients (%WISE) for the products are listed in Table 2. The mebendazole content of each product was determined using the HPLC analysis method described in the USP.<sup>23</sup>

### Polymorph Identification and Quantification

X-ray powder diffraction analysis (XRPD) was used to identify and quantify the three polymorphs of mebendazole.<sup>22</sup> XRPD patterns were recorded at ambient conditions using a Bruker D8 Advance Diffractometer (Bruker, Frankfurt, Germany). Approximately 200 mg of the powdered samples were transferred into aluminum sample holders, taking care not to induce a preferential orientation of crystals. The measurement conditions were: target, Cu; voltage, 40 kV; current, 30 mA; divergence slit, 2 mm; antiscatter slit, 0.6 mm; detector slit, 0.2 mm; monochromator; scanning speed, 2°/min (step size, 0.025°; step time, 1.0 s). XRPD patterns of the polymorphs are shown in Figure 1. The characteristic peaks used to identify and quantify the three forms are listed in Table 1. The intensities of the characteristic peaks were used to calculate the relative amounts of the polymorphs in the samples.

In addition to XRPD analysis, infrared spectroscopy (IR) was also used to identify and quantify the polymorphs. IR has emerged as the preferred method to identify the mebendazole polymorphic

forms in powders and products.<sup>9,10,19,24–26</sup> In this study IR spectra of powder samples were recorded on a Nicolet Nexus 470-FT-IR spectrometer (Nicolet, Madison, WI) over a range of 400–4000  $\text{cm}^{-1}$ . The diffuse reflectance method was used with KBr as the background material. In Table 1, the characteristic absorption bands that were used to identify and quantify polymorphs A, B, and C are listed. The AUC at the characteristic absorption bands were used to calculate the relative amounts of the polymorphs in the samples. Examples of DRIFT-IR spectra showing the conversion of form C to A are shown in Figure 2.

### Accelerated Stability Testing

First, a simple method was devised to establish the interconversion between the polymorphs when exposed to changes in temperature and moisture. To do this approximately 500 mg of the metastable mebendazole polymorphs (i.e., forms B and C) was transferred into amber glass bottles with tight-fitting caps. Water was added to half of these bottles and both the wetted and dry samples were tightly sealed. The samples were divided into three temperature groups:  $5 \pm 3$ ,  $50 \pm 3$ , and  $100 \pm 2^\circ\text{C}$ . The wetted samples and five dry samples were stored at each temperature for 75 h. Two bottles (one dry sample and one wet sample) were removed from each incubator at predetermined intervals. The wetted samples were filtered and the mebendazole residues were allowed to dry at ambient conditions for 12 h. XRPD and DRIFT-IR analysis were performed on all samples. The method described above was used for the investigation of the polymorphic stability

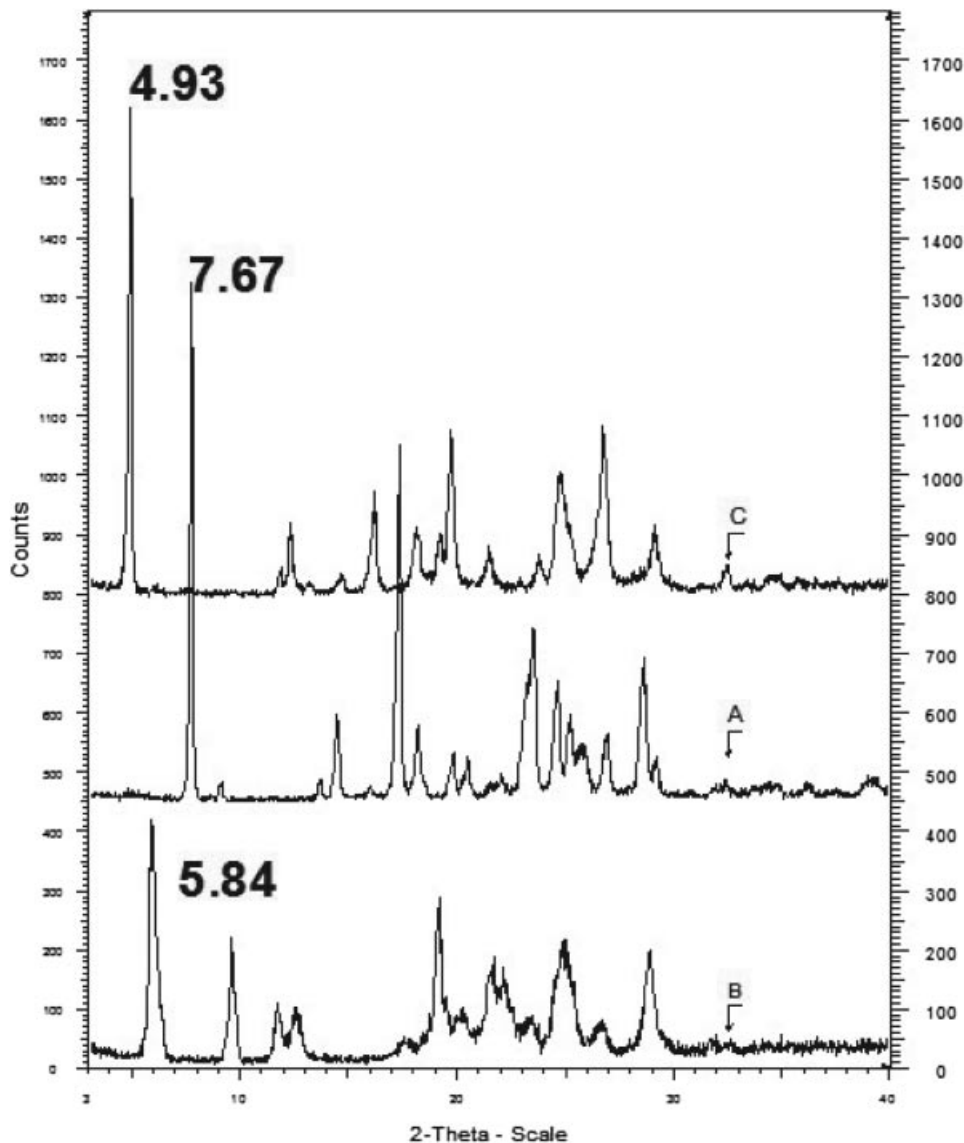


**Figure 1.** XRPD patterns of mebendazole polymorphs A, B, and C with the characteristic peak positions indicated.

of mebendazole polymorphs C and B. HPLC analysis showed that this treatment did not cause any chemical decomposition of mebendazole.

To determine possible polymorphic changes in the tablets; the various products were stored in controlled climate rooms at conditions in accordance with ICH stability guidelines for intermediate and accelerated stability testing at  $30 \pm 2^\circ\text{C}/65 \pm 5\%$  RH (climatic zones III and IV) and  $40 \pm 2^\circ\text{C}/75 \pm 5\%$  RH.<sup>27</sup> This guideline provides recommendations on stability testing protocols including temperature, humidity, and trial

duration. Furthermore, the revised document takes into account the requirements for stability testing in climatic zones III and IV in order to minimize the different storage conditions for submission of a global dossier. Tablets were stored in the original packaging. In addition, tablets of product 2 were removed from the packaging and stored in an open Petri dish. Products were tested when received and then every month for up to 6 months. XRPD and DRIFT-IR were used to evaluate the polymorphic composition of the products.

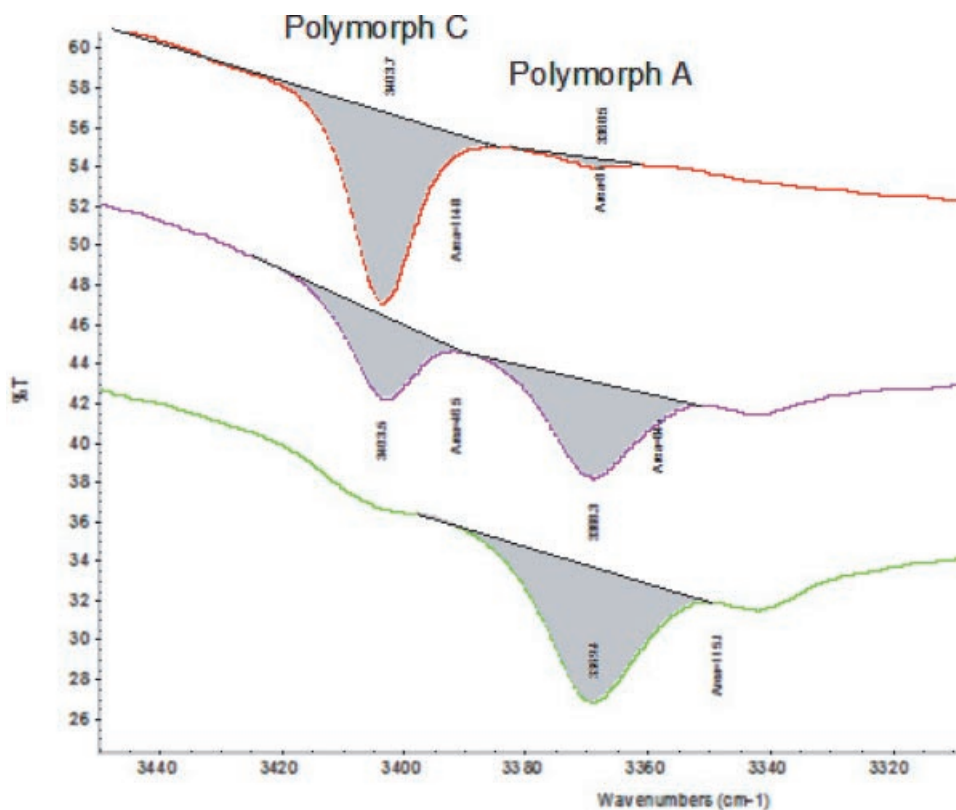


**Figure 2.** Characteristic stretching frequencies ( $\text{cm}^{-1}$ ) and the areas thereof in the DRIFT-IR spectra mebenzazole polymorphs C and A in product 3 at 0 (top), 3 (middle), and 6 (bottom) months when stored at  $40^\circ\text{C}$  and 75% RH.

### Dissolution Testing

Dissolution testing were performed on the tablets according to the USP method for mebenzazole tablets without adding sodium lauryl sulfate (SLS) to the 0.1M HCl dissolution medium.<sup>23</sup> Swanepoel et al.<sup>13,21</sup> suggested this change to the USP dissolution medium because it enables distinguishing between the active and favored polymorph C and nonfavored and inactive mebenzazole polymorphs B and A. In this medium, the percentage dissolved versus time profiles follows the order  $C > B > A$ , whereas in the USP medium the order is  $C = B = A$ .

Dissolution profiles were compared by determining the similarities between the dissolution profiles of a product after storage to that of the product at 0 months. A model-independent approach using a similarity factor first described by Moore and Flanner<sup>28</sup> and then adopted by the FDA<sup>29</sup> was used to compare profiles. This

similarity factor ( $f_2$ ) is a logarithmic reciprocal square root transformation of the sum of squared error and is a measurement of the similarity in the percent (%) dissolution between a reference and test dissolution curve calculated by

$$f_2 = 50 \times \log \left( \left[ 1 + \left( \frac{1}{n} \right) \sum_{t=1}^n w_t (R_t - T_t)^2 \right]^{-0.5} \times 100 \right) \quad (2)$$

where  $n$  is the number of time points,  $R_t$  is the dissolution value of the reference sample at time  $t$ , and  $T_t$  is the dissolution value of the test sample at time  $t$ . The value of  $f_2$  is 100 when the test and reference mean profiles are identical. Values of  $f_2$  between 50 and 100 ensure sameness or equivalence of the two curves and, thus, of the performance of the test and reference products.

## RESULTS AND DISCUSSION

### Properties of Mebendazole Polymorphs and Tablets

In Table 1, the important physicochemical and spectral properties of the three mebendazole polymorphs are listed. These properties can be measured to identify the polymorphs in raw materials and tablets. Other methods including Raman spectroscopy are also used to identify mebendazole polymorphs.<sup>30</sup> In this study XRPD, Figure 1, and DRIFT-IR analysis, Figure 2, were primarily used to identify the three polymorphs in raw materials and tablets. The characteristic peaks in the XRPD patterns of the three polymorphs, Figure 1, proved to be especially useful in following the stability of the polymorphs as shown in Figure 3. The solubilities of the mebendazole polymorphs at 30°C in 0.1M HCl, with and without added SLS, are also listed in Table 1. As reported earlier for the dissolution of mebendazole polymorphs the addition of SLS disguised the differences in solubility of the polymorphs.<sup>13,21</sup> Based on these observations the dissolution test performed on the tablets were not done in the USP dissolution medium for mebendazole tablets, but instead in 0.1M HCl. Melting point ( $T_m$ ) and heat of melting ( $\Delta H$ ) values for the polymorphs in combination with tablet excipients obtained by DSC, and listed in Table 1, were different from that reported before.<sup>22</sup> The significant variability meant that DSC was not useful in identifying mebendazole polymorphs, especially in tablets.

For this study, commercially available 100 mg mebendazole tablets from seven manufacturers with the longest possible time to expiration were obtained from local pharmacies in South Africa. Average tablet weights, mebendazole content, and moisture content (measured by Karl Fischer titration) are listed in Table 2. These results, and the results from USP dissolution testing, confirmed that the seven products complied with all pharmacopeial requirements for mebendazole tablets. XRPD diffraction analysis confirmed that all the products contained the active polymorph C. However, trace amounts of the inactive polymorph A were detected in products 1, 3, 5, and 6. Since the drug occupied around 30% of the tablets weight, roughly two-thirds of the tablets were composed of excipients, the majority most probably being the tablet diluent. For this reason XRPD analysis, Figure 4, was performed on crushed tablets and the diffraction patterns

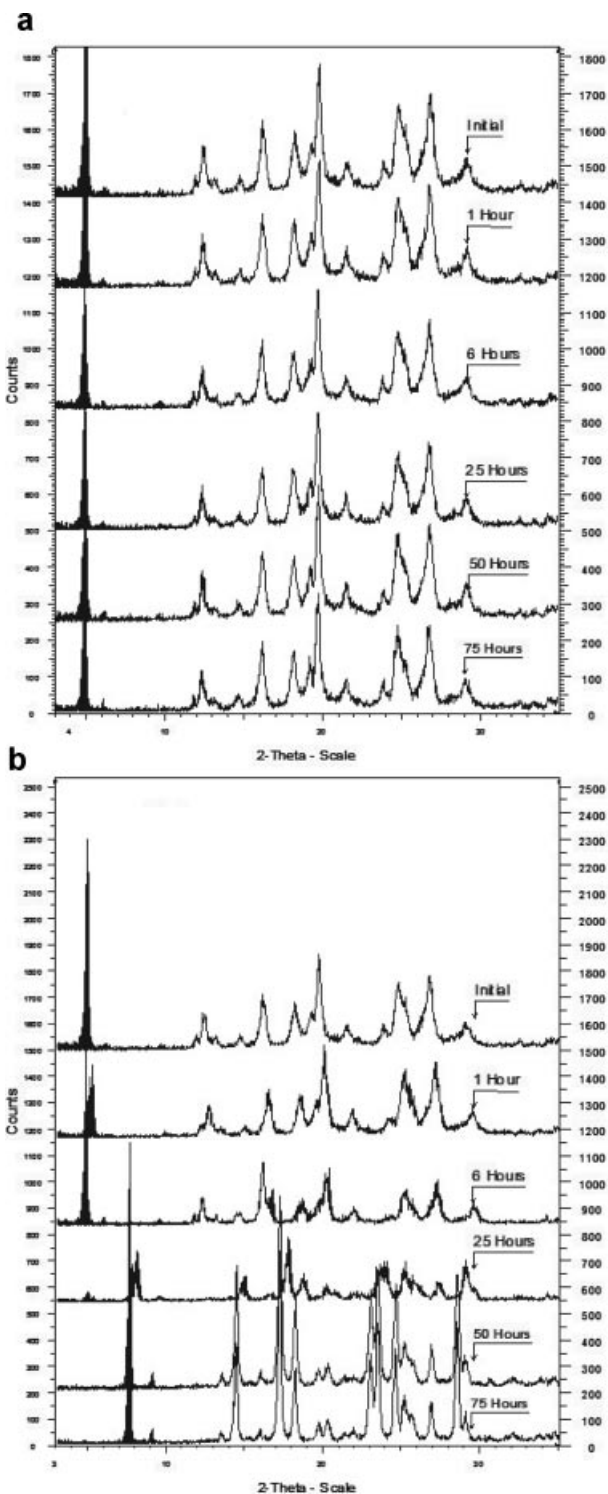


**Figure 3.** XRPD overlays of mebendazole polymorph C: (a) dried and (b) wetted samples stored at 100°C.

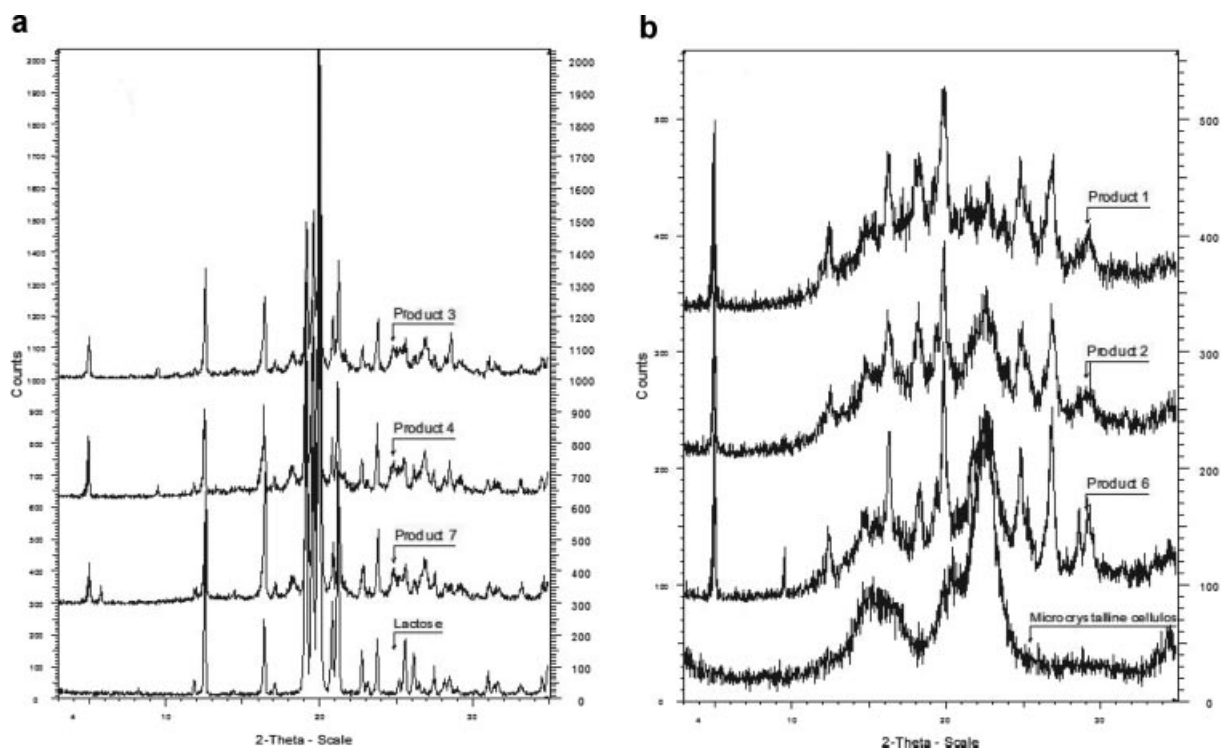


**Figure 4.** XRPD patterns of (a) product 3, product 4, product 7, and  $\alpha$ -lactose monohydrate; and (b) product 1, product 2, product 6, and microcrystalline cellulose.

compared to that of commonly used tablet diluents. As seen in Table 2, except for product 5, the tablets contained either microcrystalline cellulose (MCC) or  $\alpha$ -lactose monohydrate (Fig. 4). On average, the water-insoluble content of the tablets containing MCC was higher. After these initial tests the products were stored in controlled climate rooms in accordance with ICH stability guidelines.<sup>27</sup> The tablets were stored in the original blister packaging and the stability of the mebendazole polymorphs was investigated, using XRPD and DRIFT-IR, initially then monthly for up to 6 months. Tablets of product 2 were removed from the blister packs and stored under the same conditions.

#### Effect of Temperature and Moisture on the Stability of Mebendazole Polymorphs

Himmelreich et al.<sup>9</sup> first reported the stability of the crystal forms to be in the order  $B < C < A$ . DRIFT-IR and XRPD results showed that the exposure of mebendazole polymorph B to 5, 50, and 100°C, without moisture, for 75 h did not induce any polymorphic transitions. The position

of the  $-NH$  stretch and  $>C=O$  band was detected at 3340 and 1700  $cm^{-1}$ , respectively, which is characteristic of mebendazole polymorph B throughout the study. In addition, no traces of forms A or C were detected in any of the samples by XRPD analysis. Similarly, exposure of form C, Figure 3a, to these conditions did not induce a polymorphic transition. This correlated with the observation made earlier that form C remains stable between room temperature and  $\pm 179^\circ C$ .<sup>22</sup>

To approximate the effect of moisture on the stability of the mebendazole polymorphs, suspensions of the crystal forms in water were stored at 5, 50, and 100°C.<sup>26</sup> DRIFT-IR and XRPD analysis revealed that the suspensions of form B stored at 5°C for 75 h did not show any polymorphic transition. The DRIFT-IR spectra of the suspended form B exposed to 50°C revealed that this crystal form remained unchanged during the first 6 h of the study, and minor shoulder peaks appeared after 25 h at 3401 and 1716  $cm^{-1}$ , respectively, which suggested that a fraction of the form B transformed into form C. The XRPD patterns of the suspended samples stored at 50°C confirmed that no polymorphic transformations occurred during the first 6 h of the study but traces

of C were detected in the samples after 25 h. The relative intensities of the Bragg peak present at  $4.93 \pm 0.1^\circ 2\theta$  increased from 5.5% to 6.9% during the period 25–75 h (Fig. 1). At the end of the 75-h study, the sample consisted primarily of form B but contained traces of C (due to the presence of the small peak at  $4.93 \pm 0.1^\circ 2\theta$ ). At 100°C XRPD analysis confirmed the presence of polymorphs C, B, and A in the samples after 6 h and no traces of form B traces were detected in the 50- and 75-h samples. The XRPD pattern of the sample at 75 h resembled only that of mebendazole form A.

No changes were observed in the DRIFT-IR spectra and XRPD patterns when aqueous suspensions of form C samples were exposed to 5 and 50°C for 75 h. However, as shown in Figure 3b polymorphic transformation occurred when the suspensions were stored at 100°C for 75 h. DRIFT-IR spectra of the samples revealed significant changes during the 75 h in the 3550–3150  $\text{cm}^{-1}$  (–NH stretch) region. Initially, the sample revealed a sharp absorption peak at 3403  $\text{cm}^{-1}$ , which indicated that the sample contained form C. After 1 h, the spectrum revealed a sharp absorption peak at 3403  $\text{cm}^{-1}$  and minor peak broadening in the 3420–3440  $\text{cm}^{-1}$  region, which indicated the presence of surface moisture in the sample. The commencement of the polymorphic transformation was observed after 6 h, with the appearance of a shoulder peak at 3370  $\text{cm}^{-1}$  that indicated that the sample contained traces of mebendazole polymorph A. After 25 h the intensity of the 3403  $\text{cm}^{-1}$  peak decreased significantly and the intensity of the 3370  $\text{cm}^{-1}$  peak increased. These observations were mirrored by changes in the >C=O band (1780–1700  $\text{cm}^{-1}$ ) region and by XRPD analysis (Fig. 3b). Both DRIFT-IR and XRPD analysis showed that the 50- and 75-h samples were comparable and resembled that of form A. When suspended in water, form C transformed to form A and this change was observed at 100°C after only 6 h, and resulted in complete transformation to form A after 50 h.

### Kinetics of Mebendazole Polymorph Transformation

The fractions ( $\alpha$ ) of the individual polymorphs present in the samples suspended in water and stored at 100°C as a function of time are shown in Figure 5. For the purpose of this study the polymorph  $\alpha$  relative to the total polymorph content present in the samples were calculated

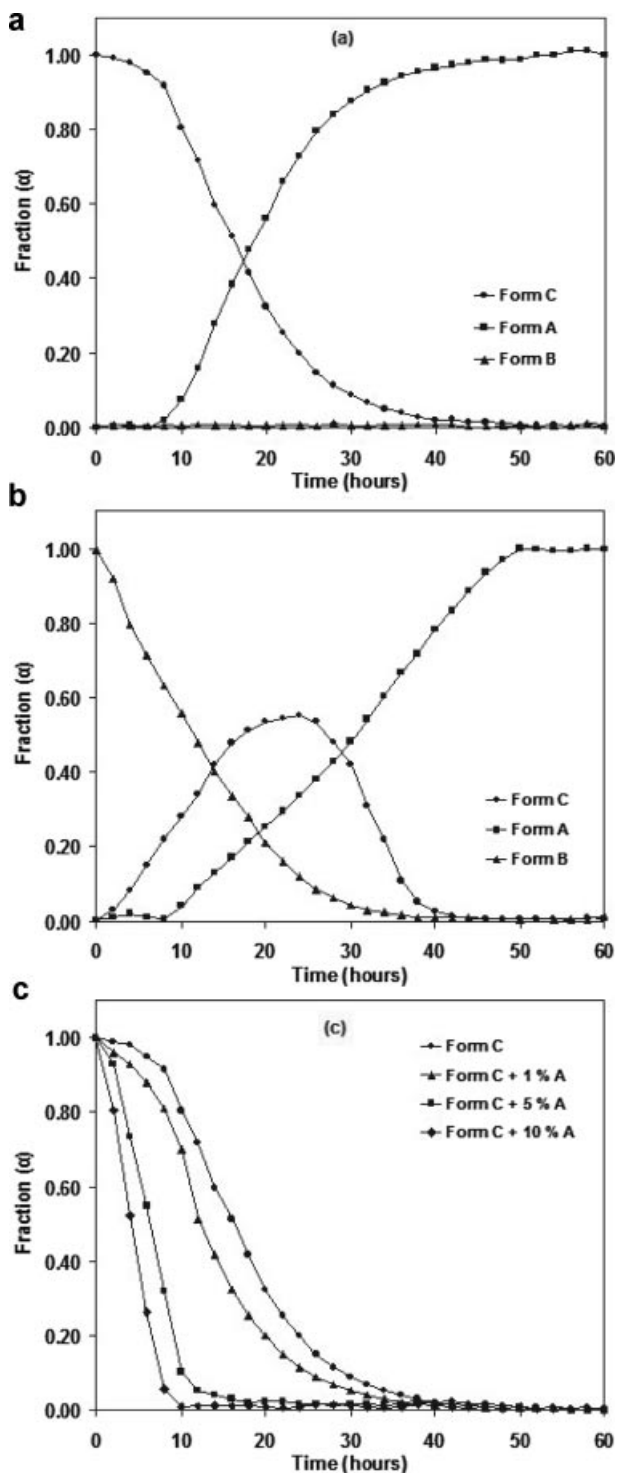


**Figure 5.** Fraction ( $\alpha$ ) of individual polymorphs present in powder samples suspended in water and stored at 100°C. (a) Polymorph C; (b) polymorph B; and (c) polymorph C containing increasing amounts of polymorph A.

from the intensities ( $i$ ) of the characteristic peaks in the XRPD patterns, Figure 1, and DRIFT-IR spectra, Figure 2 (e.g., form A  $\alpha = i_A / \Sigma(i_A, i_B, i_C)$ ). As seen in Figure 5a the decrease in form C and the increase in A followed sigmoidal paths. However, with time form B, Figure 5b, transformed to C before converting to A complicating the kinetics of this conversion. Most equations used to describe the kinetics of transformation are grouped according to the shape of the isothermal extent of transformation ( $\alpha$ ) versus time curves as acceleratory, sigmoid, or deceleratory. In the case of sigmoidal  $\alpha$ -time curves, two equations have been derived and are commonly used to describe the kinetics of such polymorphic transformations.<sup>31</sup> If the rate of the polymorphic transformation is assumed to be controlled by linearly growing nuclei that branch into chains and are terminated more rapidly as the number of nuclei increase, then the kinetics of transformation can be described by the Prout-Tompkins equation.<sup>32,33</sup>

Another very popular kinetic model applied to solid-state transformations has been the Avrami model, developed independently by several workers and thus referred to as the Johnson-Mehl-Avrami-Erofeyev-Kolmogorov (JMAEK) model.<sup>34-39</sup> The data in Figure 5 were fitted to both these models and overall the JMAEK model, Eq. (3), describe the kinetics of transformation better

$$\alpha = 1 - \exp(-kt^n) \quad (3)$$

This equation summarizes transformation kinetics for any case where  $\alpha \rightarrow 1$  as  $t \rightarrow \infty$ . Once crystallization started the characteristics of the kinetics is that of a "S-curve," that is, slow at first, then accelerating, then decelerating. Values of  $k$  and  $n$  are diagnostic of the crystallization mechanism. A useful way to analyze the kinetics of transformation is to plot the quantity  $-\log(1 - \alpha)$  versus time on a double logarithmic plot. The slope of the line is then the exponent  $n$  and the  $y$ -intercept is the log of the Avrami rate constant,  $k$ . To do this the Avrami equation can be linearized to<sup>40</sup>

$$\ln[-\ln(1 - \alpha)] = \ln k + n \ln(t) \quad (4)$$

In this study, the average value of  $n$  was  $2.01 \pm 0.27$  (Tabs. 3 and 4). The relationship between the JMAEK equation and  $n = 2$  has been reported and represents a system dominated by random nucleation and two-dimensional growth of nuclei.<sup>40</sup> Since JMAEK kinetics are a convolution of nucleation and growth kinetics it was not

**Table 3.** Accelerated Stability Parameters Calculated Using the JMAEK Model to Estimate Mebendazole Polymorph Conversions When Suspended in Water and Kept at 100°C

Polymorph	JMAEK Stability Parameters				
	$k (\times 10^{-2} \text{ h}^{-1})$	$t_{0.5} (\text{h})$	$t_{90} (\text{h})$	$n$	$r^2$
C decline	3.8	18	2.8	2.2	0.983
A growth	2.8	25	3.8	2.4	0.984
B decline	14.0	5.0	0.8	2.0	0.992
C formation	10.7	6.5	1.0	2.1	0.994
A growth	2.7	26	3.9	2.1	0.938
C + 1% A	6.7	10	1.6	1.8	0.972
C + 5% A	16.2	4.3	0.7	1.9	0.961
C + 10% A	35.7	2.0	0.3	1.8	0.965

possible to obtain any information about individual processes. However, it did allow calculation of the rate,  $k$ , of mebendazole polymorph transformation as shown in Tables 3 and 4. Rate constants were used to calculate half-lives ( $t_{0.5}$ ) and shelf lives ( $t_{0.9}$ ).

### Crystal Transformation of Polymorphs

In Table 3 the accelerated stability parameters calculated using the JMAEK model to estimate mebendazole polymorph transformations when suspended in water and kept at 100°C are listed. Some of the transformations had an induction time and for all the transformations, except for the intermediate growth of polymorph C from B,  $\alpha$  approached 1 (Fig. 5). This means that in all these cases the polymorphic transformations were almost completed within the time the tests were performed. At 100°C when suspended in water, form C rapidly transformed to form A with  $t_{0.5} = 18$  h and  $t_{0.9}$  only 3 h. For this transformation, the induction period was less than 2 h and it took about 42 h for the conversion to be completed. The growth of form A from C closely mirrored the decay of C but the growth rate was slower with  $t_{0.5} = 25$  h for the formation of A. The  $t_{0.5}$  for the decrease in form B when suspended in water at 100°C was only 5 h. Under these conditions, form B was 3.5 times less stable than form C. For form B, no induction period was observed but the time necessary for completion of the conversion was longer at around 50 h. Although form B disappeared quickly, the formation of form A from B was slow with a  $t_{0.5} = 26$ , very similar to the

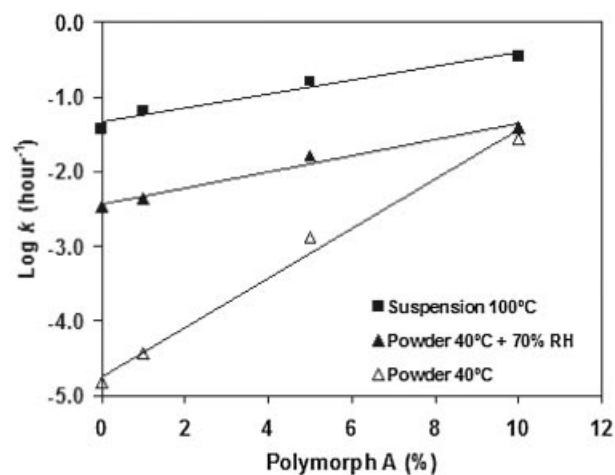
**Table 4.** Accelerated Stability Parameters Calculated Using the JMAEK Model for the Mebendazole Polymorph C to A Conversion in Commercially Available Tablets

Product	Storage Conditions	JMAEK Stability Parameters				
		$k$ ( $\times 10^{-2}$ Month $^{-1}$ )	$t_{0.5}$ (Months)	$t_{90}$ (Months)	$n$	$r^2$
1	40°C and 75% RH	2.67	26	4	1.8	0.966
2	40°C and 75% RH	0.32	217	33	2.3	0.975
2 (open)	40°C and 75% RH	1.58	44	7	2.4	0.960
3	30°C and 65% RH	6.89	10	2	1.7	0.969
3	40°C and 75% RH	8.48	8	1	1.8	0.994
4	40°C and 75% RH	0.11	630	96	2.3	0.907
5	40°C and 75% RH	2.58	27	4	1.8	0.942
6	40°C and 75% RH	2.40	29	4	1.8	0.929

half-life of the transformation of form C to A. The reason for this was that form B transformed to C, which then transformed to A. The initial rate at which form C appeared in the samples,  $0.011 \text{ h}^{-1}$ , was similar to the rate at which form B disappeared,  $0.014 \text{ h}^{-1}$ . Initially, the amount of form C increased but after about 24 h, it decreased and eventually no C was detected. This could explain why the transformation of form C is a bell-shaped curve.

Initial analysis of the tablets, Table 2, indicated that some products contained trace amounts of the unwanted polymorph A. To better understand the effect that small quantities of form A have on the transformation of form C, mixtures of the polymorphs were also studied (Fig. 5c). The rate of

transformation of form C to A in aqueous suspensions stored at  $100^\circ\text{C}$  increased with an increase in the initial content of form A from 1% to 10%. A plot of the logarithm of the rate constants,  $k$ , versus concentration of form A was linear, slope  $0.093\%^{-1}$  and  $r^2 = 0.965$ , indicating that the increase in  $k$  was first order with respect to the concentration of form A available initially (Fig. 6). This means that the addition of 1% form A doubled the rate of conversion of C to A and that the conversion rate was four times faster when adding 5% A and nine times faster when adding 10% A. Although there was on average a 11-fold reduction in the rate of transformation this same first-order increase in  $k$ , slopes  $0.093\%^{-1}$  versus  $0.108\%^{-1}$  ( $r^2 = 0.980$ ), was observed for samples stored at  $40 \pm 2^\circ\text{C}/75 \pm 5\%$  RH (Fig. 6). When powder samples were stored at  $40 \pm 2^\circ\text{C}$  the initial rate of C  $\rightarrow$  A conversion when compared to samples stored at 75% RH was about 230 times slower,  $t_{0.9} = 11$  months, for samples that did not contain A. However, with an increase in the content of form A the first-order increase in  $k$  was much faster for samples stored in the absence of moisture as shown by the difference in the slopes,  $0.108\%^{-1}$  versus  $0.329\%^{-1}$  ( $r^2 = 0.991$ ), of the fitted lines in Figure 6. In fact, for samples containing 10% A,  $k$  was not significantly different from that of samples stored at  $40^\circ\text{C} + 75\%$  RH (Fig. 6). This indicated that under controlled storage conditions the concentration of the unwanted thermodynamically most stable, least soluble, and therapeutically inactive, form A, had the greatest effect on the solid-state stability of the therapeutically active form C. Since some products contained trace amounts of form A, Table 2, this could adversely change the stability of these tablets.

**Figure 6.** The effect of an increase in the residual content of form A on the conversion of form C to form A when exposed to high temperatures and relative humidities.

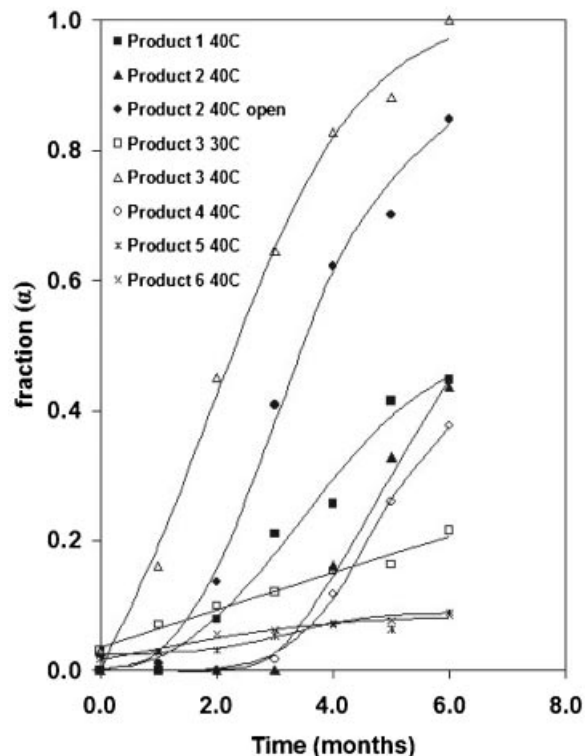


**Figure 7.** Plots showing the increase in the fraction of form A as a function of time. Lines represent the best fit of the JMAEK model, Eq. (3), with  $n = 1/2$  for each data set.<sup>40</sup> Kinetic parameters calculated from these fits are listed in Table 4.

### Crystal Transformation of Form C in Tablets

In Figure 7, the increase in the fraction of form A in the tablets is plotted as a function of time. These lines represent the best fits according to Eq. (3) with  $n = 1/2$ .<sup>40</sup> This model was also used to calculate the rate constants, half-lives, and shelf lives listed in Table 4. Data for product 7 are not shown because within the time frame of this study form A was not detected in the tablets. Although initially form A was not detected, over time some small amounts of form A was found in products 2 and 4. At 40°C + 75% RH these two products were stable in their blister packs with shelf lives ranging from 3 to 8 years. When tablets of product 2 were removed from the packaging the rate of conversion of form C → A increased fivefold reducing the shelf life to only 7 months, Table 4. This demonstrated the effect that moisture had on the polymorph transformation. Initially, products 1, 5, and 6 contained about 4–8% form A, and this significantly decreased the stability of form C in these products,  $t_{0.9} = 4$  months, when compared

to products that did not contain form A. Product 3 contained more than 10% form A and this reduced its shelf life at 40°C + 75% RH to 1 month. When this product was stored at 30°C + 65% RH its shelf life increased to 2 months. These results show that the major factor determining the stability of polymorph C at higher temperatures in blister packs is the concentration of form A present in the tablets because relatively small amounts of form A significantly reduced the stability of mebendazole tablets. These results coincided with the conclusions drawn from the accelerated stability study of the crystal forms (Tab. 3).

### Tablet Dissolution

The influence of the mebendazole polymorphic transitions on the dissolution behavior of the mebendazole tablets was investigated. The dissolution profiles were measured monthly for up to 6 months, when stored at 30°C + 65% RH and 40°C + 75% RH. Examples of the dissolution profiles are shown in Figure 8. The similarity,  $f_2$ , between the various dissolution curves (at time =  $t$ ) and that of the initially procured product (at time =  $t_0$ ) were calculated using Eq. (2). The change in the  $f_2$  values as a function of time is shown in Figure 9. Tablet dissolution was measured according to the method of the USP without adding SLS to the dissolution medium.<sup>13,21,23</sup> Initially, even without adding 1% SLS, the seven products complied with the USP tolerance of not less than 75% ( $Q$ ) of the labeled amount of mebendazole dissolved in 120 min. Mean  $Q = 86 \pm 8\%$ , min = 75 (products 3 and 4) and max = 95 (product 2). Although the  $Q$  for product 7 was only 80% dissolved in 120 min both at 30°C + 65% RH and 40°C + 75% RH this product showed the most consistent dissolution as seen in Figure 8a. The mean  $f_2$  values, Figure 9, for this product were  $94 \pm 5$  at 30°C and  $93 \pm 4$  at 40°C.

Although dissolution was decreased the  $f_2$  of products 1, 2, 4, 5, and 6 remained >50 at 30°C while that of products 1, 2, 4, and 6 remained >50 at 40°C. Products 2, 4, and 7 did not contain any trace amounts of form A initially, and this could explain the good dissolution properties. Among these products, the dissolution of product 2 at both 30 and 40°C and product 5 at 40°C was reduced the most. After 1 month the  $f_2$  values for product 2 range from 50 to 56, very close to the acceptable

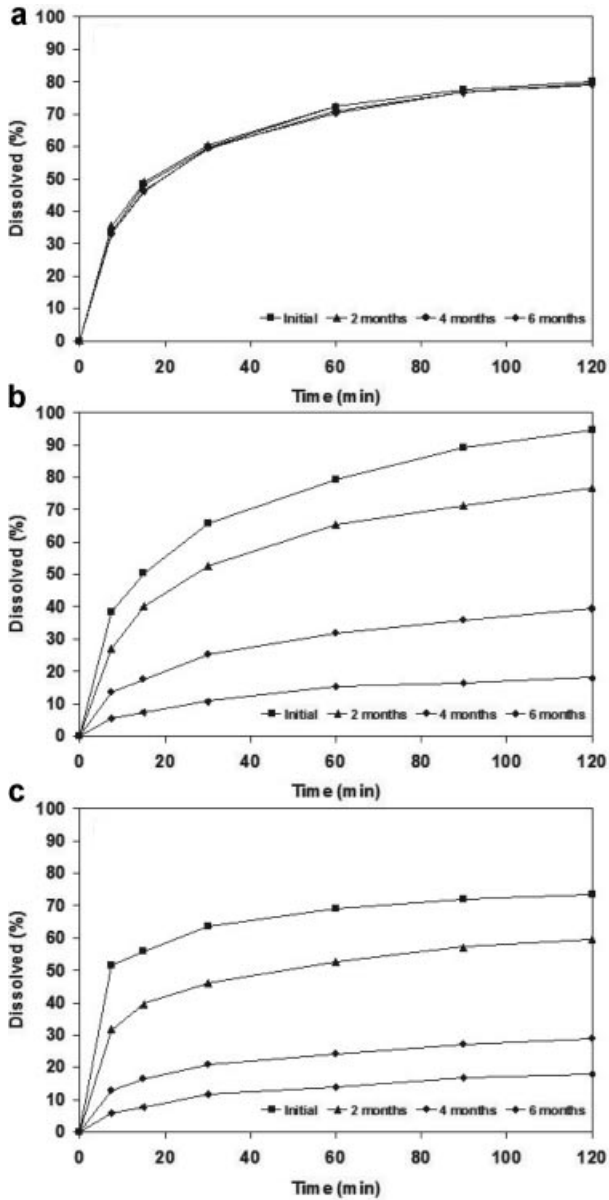


**Figure 8.** Dissolution profiles in 0.1 M HCl of mebendazole tablets stored at 40°C and 75% RH: (a) product 7; (b) product 2 open; and (c) product 3.

limit while that of product 5 dropped <50 after 4 months at 40°C. When tablets of product 2 were removed from the packaging the dissolution of mebendazole was significantly reduced as shown in Figure 8b and the  $f_2$  values dropped <50 within 3 months at both 30°C + 65% RH and 40°C + 75% RH (Fig. 9). Product 3 contained mostly form A initially and was the least stable (Tab. 4). The dissolution properties of this product was also the worst as shown in Figure 8c for tablets stored at 40°C + 75% RH. After 2 months at 30°C and

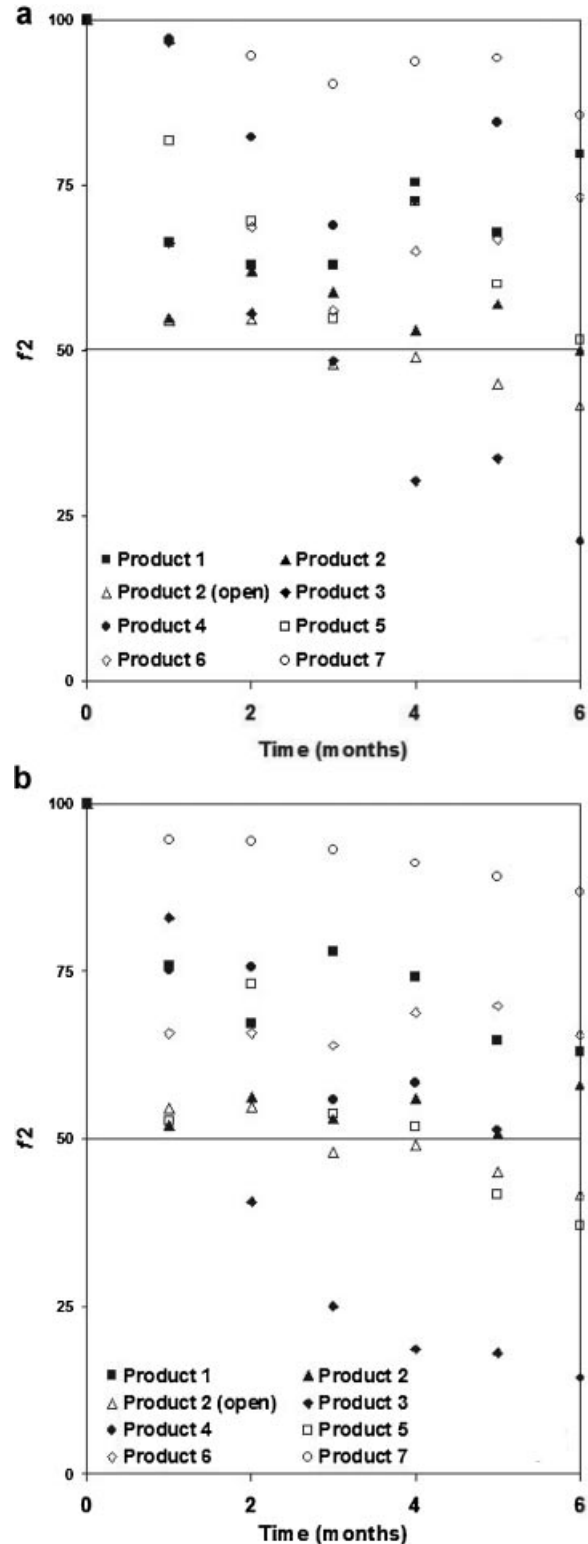


**Figure 9.** Reduction in  $f_2$  values showing how the conversion from the more soluble polymorph C to the least soluble form A lead to tablets not meeting dissolution specification,  $f_2 < 50$ . (a) Tablets stored at 30°C and 75% RH and (b) tablets stored at 40°C and 75% RH.

1 month at 40°C, the  $f_2$  values dropped <50 (Fig. 9).

A survey of package inserts and registration files available online indicated that several commercially available mebendazole tablets, including products 1, 6, and 7 used in this study, contain the surfactant SLS. The addition of this surfactant to tablets could mask the poor solubility of form A in products.<sup>13,21</sup> Still overall dissolution results indicated that those products that contained trace amounts of form A, which accelerated the transformation of form C to form A, was not only the least stable but also had the worst dissolution behavior. Especially, when the amount of form A was above 10% initially, product 3, it caused the tablets to fail the dissolution test. In addition, taking tablets that did not contain trace amounts of form A from a blister pack and exposing it to moisture rapidly led to a reduction in dissolution below acceptable limits. This showed that moisture combined with trace amounts of the thermodynamically stable polymorph A not only reduce the stability of form C in tablets but also adversely reduce dissolution and potentially the therapeutic activity of mebendazole. A problem often cited in the literature.<sup>10,14–18</sup>

## CONCLUSION

Mebendazole is a WHO essential drug available as tablets produced by many manufacturers all over the world. Several reports indicate that many of these products fail therapeutically. One reason for this is the presence of the inactive polymorph A in these tablets. In this study, we found that four out of seven products available in South Africa contained trace amounts of form A. At temperatures typically found in countries located in ICH climatic zones III (hot and dry) and IV (hot and humid) trace amounts of form A in tablets significantly accelerated the transformation of the clinically active polymorph C to form A. This transformation significantly reduced the shelf lives and the dissolution of these tablets.

## ACKNOWLEDGMENTS

We are grateful to the University of Wisconsin (USA) and the North-West University (RSA), and the National Research Foundation of South Africa (NRF) for research support.

## REFERENCES

1. Chan MS, Medley GF, Jamison D, Bundy DAP. 1994. The evaluation of potential global morbidity to intestinal nematode infections. *Parasitology* 109: 373–387.
2. Bundy DAP, Drake LJ. 2004. Intestinal helminths: The burden of disease. In: Parry E, Godfrey R, Mabey D, Gill G, editors. *Principles of Medicine in Africa*. 3rd edition. Cambridge: Cambridge University Press. pp. 386–391.
3. Stoltzfus RJ, Chwaya HM, Tielsch JM, Schulze KJ, Albonico M, Savioli L. 1997. Epidemiology of iron deficiency in Zanzibari school children: The importance of hookworms. *Am J Clin Nutr* 65:153–159.
4. Pollitt E. 1991. Effects of a diet deficient in iron on the growth and development of preschool and school-age children. *Food Nutr Bull* 13:110–118.
5. Albonico M, Allen H, Chitsulo L, Engels D, Gabrielli A-F, Savioli L. 2008. Controlling soil-transmitted helminthiasis in pre-school-age children through preventive chemotherapy. *PLoS Negl Trop Dis* 2:e126. 10.1371/journal.pntd.0000126.
6. Keiser J, Utzinger J. 2008. Efficacy of current drugs against soil-transmitted helminth infections. Systematic review and meta-analysis. *J Am Med Assoc* 299:1937–1948.
7. Montresor A, Awashti S, Crompton DWT. 2003. Use of benzimidazoles in children younger than 24 months for the treatment of soil-transmitted helminthiasis. *Acta Trop* 86:223–232.
8. Montresor A, Stoltzfus RJ, Albonico M, Tielsch JM, Rice AL. 2002. Is the exclusion of children under 24 months from anthelmintic treatment justifiable? *Trans R Soc Trop Med Hyg* 96:197–199.
9. Himmelreich M, Rawson BJ, Watson TR. 1977. Polymorphic forms of mebendazole. *Aus J Pharm Sci* 6: 123–125.
10. Costa J, Fresno M, Guzman L, Igual A, Oliva J, Vidal P, Perez A, Pujol M. 1991. Polymorphic forms of mebendazole: Analytical aspects and toxicity. *Circ Farm* 49:415–424.
11. Kumar S, Chawla G, Sobhia ME, Bansal AK. 2008. Characterization of solid-state forms of mebendazole. *Pharmazie* 63:136–143.
12. Hadkar UB, Ektare AA. 1998. Diffusion studies on mebendazole polymorphs. *Indian Drugs* 35:98–102.
13. Swanepoel E, Liebenberg W, Devarakonda B, De Villiers MM. 2003. Developing a discriminating dissolution test for three mebendazole polymorphs based on solubility differences. *Pharmazie* 58:117–121.
14. Lopatin BV, Krotov AI, Dzhabarova VI. 1985. Polymorphism and chemotherapeutic action of mebendazole. *Med Parazitol (Mosk)* 5:51–53.
15. Ren H, Cheng B, Ma J, Hua D. 1987. Comparative effectiveness of mebendazole with different poly-

- morphic forms against *Nippostrongylus braziliensis*. *Yiyao Gongye* 18:356–359.
16. Rodriguez-Caabeiro F, Criado-Fornelio A, Jimenez-Gonzalez A, Guzman L, Igual A, Perez A, Pujol M. 1987. Experimental chemotherapy and toxicity in mice of three mebendazole polymorphic forms. *Chemotherapy* 33:266–271.
  17. Charoenlarp P, Waikagul J, Muennoo C, Srinophakun S, Kitayaporn D. 1993. Efficacy of single-dose mebendazole, polymorphic forms A and C, in the treatment of hookworm and *Trichuris* infections. *Southeast Asian J Trop Med Public Health* 24:712–716.
  18. Evans AC, Fincham JE, Dhansay MA, Liebenberg W. 1999. Anthelmintic efficacy of mebendazole depends on the molecular polymorph. *S Afr Med J* 89:1118.
  19. Liebenberg W, Dekker TG, Lotter AP, De Villiers MM. 1998. Identification of the mebendazole polymorphic form present in raw materials and tablets available in South Africa. *Drug Dev Ind Pharm* 24:485–488.
  20. Froehlich PE, Gasparotto FS. 2005. Mebendazole: Identification of polymorphic forms in different bulk substance and dosage formulations (reference and generic) available in the Brazilian market. *Rev Ciênc Farm Básica Apl* 26:205–210.
  21. Swanepoel E, Liebenberg W, De Villiers MM. 2003. Quality evaluation of generic drugs by dissolution test: Changing the USP dissolution medium to distinguish between active and non-active mebendazole polymorphs. *Eur J Pharm Biopharm* 55:345–349.
  22. De Villiers MM, Terblanche R, Liebenberg W, Swanepoel E, Dekker TG, Song M. 2005. Variable-temperature X-ray powder diffraction analysis of the crystal transformation of the pharmaceutically preferred polymorph C of mebendazole. *J Pharm Biomed Anal* 38:435–441.
  23. USP 30, 2007. The United States Pharmacopeial Convention, Inc., Rockville.
  24. Bunaciu AA, Fleschin S, Aboul-Enein HY. 2001. Analysis of mebendazole polymorphs by Fourier transform infrared spectrometry using chemometric methods. *Spec Lett* 34:527–536.
  25. Chen Y, Xuan J, Ma J. 1992. IR matrix determination of polymorphic forms of mebendazole. *Zhongguo Yiyao Gongye Zazhi* 23:496–498.
  26. Agatonovic-Kustrin S, Glass BD, Mangan M, Smithson J. 2008. Analysing the crystal purity of mebendazole raw material and its stability in a suspension formulation. *Int J Pharm* 361:245–250.
  27. ICH: Q1A(R2). 2003. Stability testing of new drug substances and products (second revision). Fed Regist 68:65717–65718.
  28. Moore JW, Flanner HH. 1996. Mathematical comparison of curves with an emphasis on in vitro dissolution profiles. *Pharm Tech* 20:64–74.
  29. FDA. 1997. Center for Drug Evaluation and Research, Guidance for Industry: Dissolution Testing of Immediate Release Solid Oral Dosage Forms. <http://www.fda.gov/cder/guidance/1713bp1.pdf>.
  30. Ayala AP, Siesler HW, Cuffini SL. 2008. Polymorphism incidence in commercial tablets of mebendazole: A vibrational spectroscopy investigation. *J Raman Spec* 39:1150–1157.
  31. Byrn SR, Pfeiffer RR, Stowell JG. 1999. Solid-state chemistry of drugs. West Lafayette, IN: SSCI, Inc. p. 575.
  32. Prout EG, Tompkins FC. 1946. Thermal decomposition of silver permanganate. *Trans Faraday Soc* 42:468–472.
  33. Brown ME, Glass BD. 1999. Pharmaceutical applications of the Prout-Tompkins rate equation. *Int J Pharm* 190:129–137.
  34. Kolmogorov AA. 1937. Statistical theory for the recrystallization of metals. *Bull Acad Sci* 1:355–359.
  35. Johnson W, Mehl R. 1939. Reaction kinetics in processes of nucleation and growth. *Trans Am Inst Min Metall Eng* 135:416–446.
  36. Avrami M. 1939. Kinetics of phase change. I: General theory. *J Chem Phys* 9:1103–1112.
  37. Avrami M. 1940. Kinetics of phase change. II: Transformation-time relations for random distribution of nuclei. *J Chem Phys* 8:212–224.
  38. Avrami M. 1941. Kinetics of phase change. III: Granulation, phase change, and microstructures. *J Chem Phys* 9:177–184.
  39. Erofeev BV. 1946. Generalized equation of chemical kinetics and its application in reactions involving solids. *Compt Rend Acad Sci USSR (Dokl Akad Nauk SSSR)* 52:511–514.
  40. Hancock JD, Sharp JH. 1972. Method of comparing solid-state kinetic data and its application to the decomposition of kaolinite, brucite, and barium carbonate. *J Am Cer Soc* 55:74–77.